



**GEOCHEMISTRY OF BANDED IRON FORMATIONS (HEMATITITE AND ITABIRITE, QUADRILÁTERO FERRÍFERO, BRAZIL**

M. Selmi<sup>1\*</sup>; L. E. Lagoeiro<sup>2</sup>; I. Endo<sup>3\*\*</sup>

<sup>1</sup>Depto. de Geologia, Universidade Federal de Ouro Preto – UFOP, Campus Morro do Cruzeiro s/nº, CEP 35.400-000, Ouro Preto, MG, Brazil, phone: +55-31-3559-1683. fax: +55-31-3559-1606

<sup>2</sup>Depto. de Geologia, Universidade Federal de Ouro Preto – UFOP, Campus Morro do Cruzeiro s/nº, CEP 35.400-000, Ouro Preto, MG, Brazil

<sup>3,2</sup>Depto. de Geologia, Universidade Federal de Ouro Preto – UFOP, Campus Morro do Cruzeiro s/nº, CEP 35.400-000, Ouro Preto, MG, Brazil, phone +55-31-3559-1853

E-mail: \*selmi@degeo.ufop.br (autor para correspondência); \*\*issamu@degeo.ufop.br

Recebido em: 07/08, aprovado para publicação em 03/09

**ABSTRACT**

*21 samples of hematitite and 12 samples of itabirite were collected through different parts of Quadrilátero Ferrífero (QF) area and were analysed for minor elements with the purpose to understand the source of banded iron formation (BIF). Hematite is the main iron phase and magnetite appears as relict. Tourmaline appears sporadically in minor or trace amounts. Trace element concentrations are relatively low with considerable variability and present anomalous values. REE abundance is relatively low. Chondrite normalized pattern shows relatively high degree of fractionation of LREE to HREE and slight positive Eu anomaly similar to some patterns of BIFs around the world. These features suggest a hydrothermal source of iron. Metamorphic overprinting in the eastern domain suggest supergene enrichment model for QF iron formation origin indicated by anomalous values of minor elements. The source for iron might be near the eastern part of QF region indicated by high values of (La/ Yb)<sub>N</sub> ratio.*

**RESUMO**

*Foram coletadas 21 amostras de hematitito e 12 de itabirito em diferentes pontos do Quadrilátero Ferrífero (QF) e a partir de análises geoquímicas foram obtidos dados referentes aos elementos menores com o objetivo de caracterizar a fonte da formação ferrífera bandada. A hematita é a principal fase de ferro e a magnetita aparece como relictos. A turmalina aparece esporadicamente em quantidades menores ou traço. A concentração de elementos traço nas formações ferríferas e nas amostras de hematita são relativamente baixas com considerável variabilidade e mostram valores anômalos. A abundância de REEs é relativamente baixas. O padrão normalizado por condrito mostra grau de fracionamento relativamente leve alto de ETRleves a ETRpesados e anomalias positivas leves de Eu semelhantes a alguns padrões de BIFs ao redor do mundo que*

sugerem fonte hidrotermal. O grau de metamorfismo no domínio oriental levou ao modelo de enriquecimento supergênico para a origem da formação de ferro de QF, sugerida por valores anômalos de elementos menores. A fonte dos elementos componentes das formações ferríferas encontra-se a leste da região, indicado pelo alto valores da  $(La/Yb)_N$ .

## INTRODUCTION

The Quadrilátero Ferrífero (QF) comprises an approximately square area of ca. 7.000 km<sup>2</sup> and hosts one of the largest iron ore deposit in the world (Figure1).

Researchers have focused on trace and rare earth elements to reveal the origin of classical Iron Formations (IFs) around the world such as the Algoma and Lake Superior-type (Gross, 1980), Hamersley in western Australia (Alibert and Mcculloch,

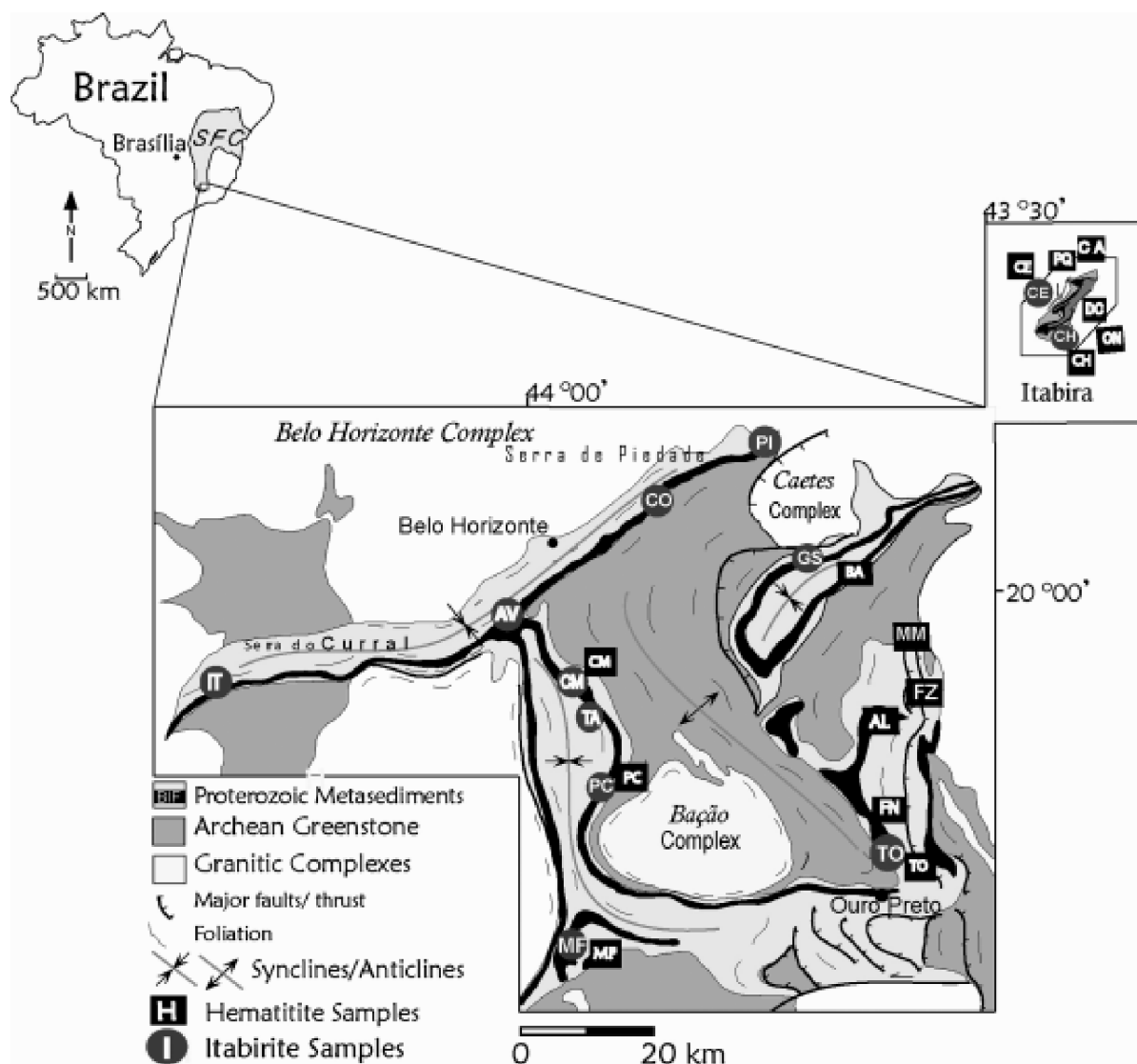


**Figure 1:** Simplified geological map of the Quadrilátero Ferrífero (after Dorr, 1969), (SFC) São Francisco Cráton. Sampled iron ore deposits: IT – Itatiaiuçu, AV – AVG Mineração, CO – Córrego do Meio, PI – Piedade, CM – Capitão do Mato, TA – Tamanduá, PC – Pico do Itabirito, MF – Mina de Fábrica, GS – Gongo Soco, BA – Baú, MM – Morro da Mina, FZ – Fazendão, AL – Alegria, FN – Fábrica Nova, TO – Timbopeba, CE – Mina de Conceição, PQ – Mina do Periquito, DC – Mina de Dois Córregos, ON – Mina do Onça, CH – Mina da Chacrinha, CA – Mina de Cauê.

1993), Kuruman and Penge in South Africa (Bau and Dulski, 1996), Maru IF in Nigeria (Adekoya, 1998) and IF from Sargur Belt in India (Kato *et al.*, 1996). However, studies on Ifs in Brazil are very scarce. Klein and Ladeira (2000) studied IFs of the western QF region which are similar to the metamorphosed banded iron formation in North America, and in Brazil they are known as itabirite-IFs. Based on trace and rare-earth element contents of the analysed itabirites they postulated an origin for the Quadrilátero Ferrífero Iron Formations (QF-IFs) by precipitation from mixed Paleoproterozoic seawater and hydrothermal fluids. Dolomitic tabirite rocks were investigated by Spier *et al.* (2007) in terms of the total concentration of trace and rare-earth elements. They proposed a similar origin for the Ifs from the north of the QF with minor or negligible terrigenous influx. In the QF two main types are of broad distribution: the itabirite and hematitite and they are the main iron ores exploited in the QF mines. With the purpose of contributing to understand the geochemical characteristics of the itabirite. Whole-rock analyses of representative samples from different deposits have been done. The samples were separated in two distinct types: hematitite and itabirite depending on their chemical composition. The term itabirite is defined as a laminated, metamorphosed oxide facies IF in which the original chert bands have been recrystallized into granular quartz followed by segregation of iron phases in thin layers giving rise to the compositional banding of the IFs (Dorr and Barbosa, 1963). Hematitite is a high grade iron ore containing more than 90% of hematite in the modal proportion. Trace and rare earth elements were analysed in terms of its spatial distribution variation in samples of the same or different types, as well as to put some constrains on their origin and possible location of the source of Fe based on trace and REE geochemistry.

### **Geologic Setting**

Samples analysed in this study belong to the hematite-magnetite lithofacies

of Iron Formation (IF) in the Quadrilátero Ferrífero (QF) region which is located in southern part of São Francisco Craton (Dorr, 1969) (Figure 1). Two broad compositional types of iron formations occur in the QF area: quartzitic and dolomitic itabirite. IFs of amphibolitic composition can also be found in the QF area although in much less proportions and restricted to thin horizons in some locations (Dorr, 1969). In this paper only samples of iron oxide lithofacies were analysed. The Cauê Formation (age between 6 and 2.4 Ga.) and the overlying Gandarela Formation of the Itabira Group were deposited over an Archean sialic substrate (Cordani *et al.*, 1980; Marshak and Alkmim, 1989) in a continental platform of a passive margin (Marshak and Alkmim, 1989).

The tectonic and metamorphic history of the QF region is controversial. At least two main tectonic events occurred in the area during the Proterozoic. The first is the Transamazonian event (ca 2.1 Ga, Alkmim and Marshak 1998) that generated large northeast-trending regional-scale folds in the QF area (Figure 1). The second is the Brasiliano Orogeny (ca 600 Ma) generating a series of west vergent thrust-and-fault structures associated with the development of pervasive tectonic fabrics (schistosity, mylonitic foliations, crenulation cleavage and mineral stretching lineations) (Chemale *et al.*, 1994).

The QF region has been usually divided into two major tectonic domains (Rosière *et al.*, 2001). The eastern region is considered as high strain domain with a widespread shear zone development and pervasive structures. By contrast, the deformation style in the western portions is a typical low strain domain. Synclines are preserved and primary structures can be recognized.

The metamorphic grade also increases from the west (lower greenschist facies) to the east (lower amphibolite facies) (Herz, 1978; Pires, 1995). The mineral assemblage indicates temperatures ranging

f

from 300°C in the west region to 600°C in the east (Pires, 1995).

### **Mineralogy and petrography**

The analysed iron-rich rocks comprise hematite and itabirite (Figure 2). The difference between them is the proportion of iron oxide to quartz. The mineral composition of both sample types is characteristically simple. By far the major constituent minerals are hematite, magnetite and quartz. Occasionally, minor to trace amounts of tourmaline, apatite and few other silicates, such as amphiboles, may be present, particularly in lfs of the western domain of the QF region. The hematite is composed basically of hematite (Figure 2a, b). Magnetite is also present in varied amounts depending on the location of sampling. It is most commonly found in the western domain of the QF area (Rosière, 2001). There magnetite of primary grade (original) and this area characterized by low grade of metamorphism which is not able to change the original chemical composition of rock (Lagoeiro, 1998; Rosière *et al.*, 2001). The magnetite grains progressively become rare in iron formation towards the east domain of the QF because they are transformed to hematite. They are only observed as relict grains immersed in a matrix of hematite crystals. There magnetite crystals are mostly euhedral and in a large extent oxidized to hematite (Figure 2c). By contrast hematite grains occur in a great variety of shapes. They can be granular (Figure 2d) with irregular or straight boundaries. Hematite grains of tabular or platy shape (Figure 2e) are more often observed in domains of high strain in the QF, particularly in the eastern domain. Hematite grains in these rocks show a strong shape and crystallographic preferred orientation (Morales *et al.*, 2008). For that reason hematite are very well foliated and occur mainly in areas of intense deformation.

On the other hand, itabirite (Figure 2f) has a remarkable compositional banding of

alternating layers of iron oxide and quartz of variable thicknesses. The proportion of iron oxides and quartz in each layer may vary in wide proportions. However pure oxide layers are essentially composed of hematite in granular, tabular or platy shapes. The microstructures of hematite grains in these layers may vary from aggregates of randomly oriented crystals to those where basal planes of hematite are preferred oriented usually defining a plane of foliation similar to that of micas (Figure 2g). In general grain sizes tend to be smaller in the iron formation of the western domain than in their counterparts of the eastern domain.

### **METHODOLOGY**

21 samples of hematite (high grade hematite ores) and 12 of itabirite were analysed for trace and rare earth elements. We have analysed only cohesive and fresh samples, e.g. those without any sign of weathering collected in deep open pit mine. Hematite samples are chemically more homogeneous even though in some specimens a contrasting arrangement of hematite crystals disposed in alternating bands gives rise to a planar anisotropy similar to those of the itabirite. The samples were cleaned and dried and then crushed to 150 mesh size in a tungsten carbide ringmill. The fine fraction pulverized samples were sent to the ACME Analytical Laboratories Ltd. (Vancouver, BC, Canada) for geochemical analyses. Major and trace elements Zr and Y were determined by wavelength dispersive, sequential X-ray fluorescence spectrometer. Selected trace (V, Co, Ni, Cu, Zn, Rb, Sr, Ba, Hf and Ta) and rare-earth elements were determined by inductively coupled plasma mass spectrometry (ICP-MS) at ACME Lab. The limit of detection of trace elements is > 0.5 ppm for the group (Hf, Nb, Rb, Sr, V, Co), the limit is > 0.1 for the group (Y, Ta) and 1 ppm for Sn whereas the limit of detection of Rare earth elements is > 0.05 ppm for (Eu, Gd, Tb, Dy, Yb, Tm, Er, Ho, Lu) while the limit is > 0.1 ppm for Sm and > 0.4 ppm for Nd.

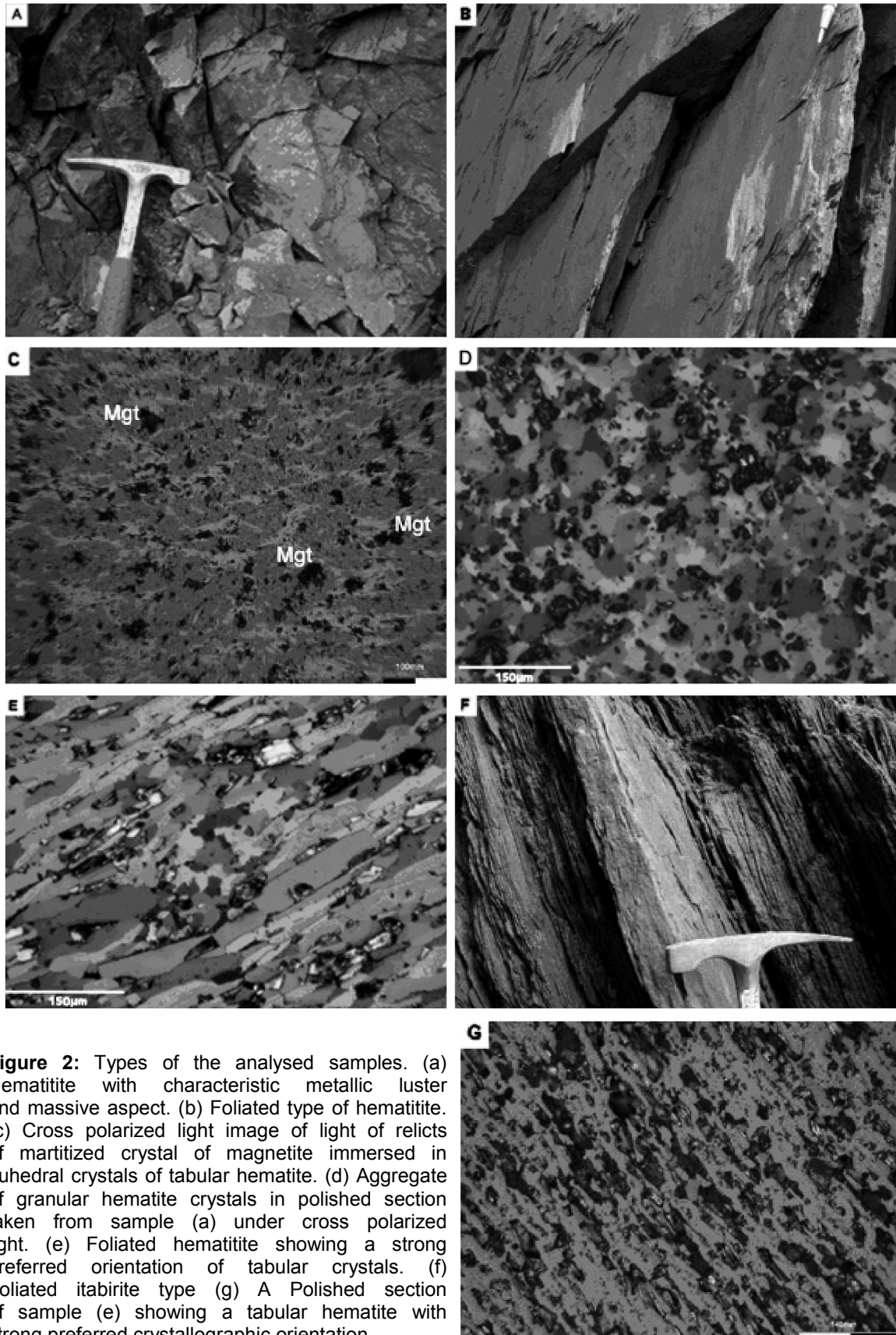


**Figure 2:** Types of the analysed samples. (a) Hematite with characteristic metallic luster and massive aspect. (b) Foliated type of hematite. (c) Cross polarized light image of light of relicts of martitized crystal of magnetite immersed in euhedral crystals of tabular hematite. (d) Aggregate of granular hematite crystals in polished section taken from sample (a) under cross polarized light. (e) Foliated hematite showing a strong preferred orientation of tabular crystals. (f) Foliated itabirite type (g) A Polished section of sample (e) showing a tabular hematite with strong preferred crystallographic orientation.

**RESULTS**

**Trace elements (TE)**

Thirteen trace elements (V, Co, Ni, Cu, Zn, Rb, Sr, Y, Zr, Nb, Ba, Hf and Ta) were determined in the hematitite and itabirite samples (Table 1). In both ores the trace element contents present a wide range of concentrations similar to the other IFs around the world (Cole, 1981; Adekoya, 1998). Both samples, hematitite and itabirite

have similar concentration all over the QF region as shown in (Figure 3).

In the hematitite samples the abundance of the trace elements varies between ca. 23.6-262 ppm. Most individual trace elements show wide concentrations. V is the most abundant with an average of 39 ppm. Co (9 ppm) Ni (5.5 ppm) and Y contents (8.2 ppm) also present a wide range of values (1-45.8 ppm). In lower range of values appear Rb (0.3-6 ppm), Sr (0.3-22.7 ppm), Zr (1.7-25.1 ppm), Nb (0.3-11.3 ppm), Hf (0.3-0.6 ppm)

**Table 1:** Trace and rare earth elements of hematitite and itabirite samples, (trace and rare earth elements in ppm); (H) hematitite, (I) itabirite, the rest of sample name refer to the mines listed in figure 1.

TRACE ELEMENTS - HEMATITITE											
ppm	HMF	HPC	HCM	HBA	HFN1	HFN2	HAL1	HAI2	HMM1	HMM2	HFZ1
V	37	18	57	69	17	2.5	42	57	10	8	96
Co	4.7	14.3	3.8	6.6	14.2	5.8	11.3	20.9	6.0	4.5	5.6
Ni	37.3	6.3	30.7	1.7	4.0	0.9	2.6	13.8	1.5	4.2	1.4
Cu	6.2	0.9	7.8	2.0	0.6	0.5	2.9	3.5	0.5	1.9	0.1
Zn	5	3.0	6.0	3.0	2.0	1.0	2.0	50	2.0	3.0	1.0
Rb	0.3	0.7	0.6	0.3	0.3	0.3	0.3	0.3	0.3	0.7	0.3
Sr	5.8	1.6	10.2	8.1	1.0	0.3	3.7	22.7	0.3	0.9	3.7
Y	9.2	2.8	10.6	3.1	3.4	8.6	13.5	46.8	7.4	6.0	16.8
Zr	2	4.1	4.4	3.4	9.5	3.6	1.7	25.1	4.4	3.7	4.0
Nb	11.3	0.3	9.2	0.3	0.6	0.3	0.3	1.8	0.3	0.3	0.3
Ba	2.9	2.2	28.3	32.3	7.8	1.9	5.8	11	8.2	7.3	4.2
Hf	0.3	0.3	0.3	0.3	0.3	0.3	0.3	0.3	0.3	0.3	0.3
Ta	0.1	0.2	0.1	0.1	0.1	0.1	0.2	0.1	0.1	0.1	0.1
ΣTE	122	54.7	169	130	60.8	23.6	86.6	262	41.3	32.9	133

TRACE ELEMENTS - HEMATITITE												
ppm	HTO	HCE	HPQ1	HPQ2	HDC1	HDC2	HCH	HCA	HON	MIN	MAX	AVG
V	37	48	43	37	74	37	22	25	18	2.5	96	39
Co	6.3	20.3	6.6	2.3	5.2	9.2	11.3	6.6	4.8	2.3	20.9	9
Ni	1.8	0.9	1.0	1.0	0.9	0.4	1.1	0.3	0.2	0.2	37.3	5.5
Cu	2.3	0.3	4.6	10.5	1.9	2.4	3.4	1.8	1.6	0.1	10.5	2.9
Zn	1.0	1.0	1.0	1.0	2.0	1.0	1.0	0.5	0.1	0.1	50.0	4.4
Rb	0.3	0.3	0.3	0.3	0.3	0.3	0.3	0.3	0.3	0.3	6.0	0.6
Sr	2.8	1.4	1.3	1.9	2.7	1.0	3.8	0.5	0.3	0.3	22.7	3.7
Y	4.7	7.9	4.4	1.1	9.3	2.7	2.1	4.3	1.0	1.0	45.8	8.2
Zr	2.7	11.4	2.3	3.9	18.8	12.7	6.2	4.7	3.3	1.7	25.1	7.0
Nb	0.3	0.3	0.3	0.3	0.9	0.3	0.3	0.3	0.3	0.3	11.3	1.4
Ba	2.8	35.2	12.1	12.3	7.7	28.5	4.2	0.3	0.9	0.3	35.2	10.8
Hf	0.3	0.3	0.3	0.3	0.3	0.3	0.3	0.3	0.3	0.3	0.6	0.3
Ta	0.1	0.3	0.3	0.1	0.1	0.2	0.1	0.1	0.1	0.1	0.3	0.1
ΣTE	62.4	128	77.5	72	124	96	56.1	45	31.2	23.6	262	92.6

HEMATITITE (REE Concentrations)												
ppm	HMF	HPC	HCM	HBA	HFN1	HFN2	HAL1	HAI2	HMM1	HMM2	HFZ1	HFZ2
La	2.4	2	2.7	1	2.8	0.5	3.1	39.9	3.1	4.5	2	5.4
Ce	5	3.7	4.7	1.4	3.1	0.9	6.9	104	3.2	3.9	6.6	9
Pr	0.73	0.36	0.5	0.17	0.55	0.13	1.04	9.44	0.55	0.67	0.61	0.9
Nd	3.2	0.9	2.4	1.4	1.8	0.4	4.2	33.5	2.6	2.5	2.6	3
Sm	1	0.3	0.6	0.2	0.3	0.2	1.3	6.5	0.4	0.4	1.2	0.8
Eu	0.27	0.08	0.23	0.1	0.09	0.08	0.45	1.51	0.12	0.14	0.41	0.4
Gd	1.23	0.22	1.02	0.32	0.26	0.24	1.51	4.41	0.4	0.49	1.36	0.8
Tb	0.2	0.05	0.16	0.06	0.03	0.08	0.24	0.78	0.08	0.09	0.26	0.1
Dy	1.07	0.37	1.14	0.35	0.29	0.58	1.42	4.92	0.67	0.54	1.55	0.9
Ho	0.29	0.07	0.26	0.08	0.06	0.17	0.35	1.09	0.16	0.1	0.38	0.2
Er	0.8	0.22	0.77	0.21	0.25	0.55	1.01	3.23	0.63	0.44	1.36	0.9
Tm	0.12	0.05	0.15	0.05	0.05	0.11	0.17	0.58	0.11	0.06	0.22	0.2
Yb	0.87	0.35	0.86	0.24	0.34	0.59	0.91	3.36	0.86	0.44	1.35	1.2
Lu	0.12	0.16	0.03	0.48	0.08	0.15	0.04	0.05	0.03	0.06	0.07	0.2
ΣLREE	13.8	7.56	12.1	4.65	8.93	2.53	18.7	199	10.4	12.6	15	20.3
ΣHREE	3.27	1.17	3.21	1.05	0.73	1.57	2.48	14	1.79	1.1	3.38	3.6
ΣREE	17.3	8.78	15.5	6.06	9.95	4.68	22.6	213	12.9	14.3	19.9	24
Eu/Eu*	1.1	1.4	1.35	1.8	1.7	1.5	1.5	1.3	1.4	1.5	1.5	2
(La/Sm) <sub>N</sub>	2.4	6.7	4.5	5	2.5	9.3	2.4	6.1	7.8	11.3	1.7	6.8
(Gd/Yb) <sub>N</sub>	1.4	0.6	1.2	1.3	0.3	0.8	1.7	1.3	0.5	1.3	1	0.7
(La/Yb) <sub>N</sub>	2.8	5.7	3.1	4.2	0.8	8.2	3.4	11.7	3.6	11.3	1.5	4.5
(Sm/Yb) <sub>N</sub>	1.2	1.0	0.77	0.95	0.6	1.0	1.6	3.3	0.7	1.1	1.8	0.9
HEMATITITE (REE Concentrations)												
ppm	HTO	HCE	HPQ1	HPQ2	HDC1	HDC2	HCH	HCA	HON	MIN	MAX	AVG
La	14.3	1.6	5.8	4.2	4.2	2.1	0.7	0.9	0.7	0.5	39.9	6.51
Ce	22.8	2.8	3.7	6.7	7.2	3.7	1.2	1.4	1.3	0.9	104	13.9
Pr	2.83	0.27	1	0.79	0.91	0.6	0.16	0.18	0.14	0.13	9.44	1.45
Nd	11.5	1	4.3	3.1	4.1	2.8	0.6	0.4	0.4	0.4	33.5	5.46
Sm	2	0.3	0.9	0.8	1.1	0.5	0.2	0.2	0.1	0.2	6.5	1.22
Eu	0.5	0.06	0.14	0.2	0.4	0.1	0.05	0.06	0.05	0.06	1.51	0.34
Gd	1.65	0.2	0.71	0.69	1.17	0.4	0.25	0.38	0.05	0.2	4.41	1.04
Tb	0.26	0.05	0.09	0.08	0.2	0.1	0.05	0.05	0.01	0.01	0.78	0.17
Dy	1.05	0.31	0.56	0.37	1.12	0.5	0.27	0.4	0.09	0.09	4.92	1.04
Ho	0.16	0.1	0.12	0.05	0.25	0.1	0.05	0.07	0.05	0.05	1.09	0.25
Er	0.45	0.33	0.36	0.12	0.73	0.2	0.15	0.26	0.05	0.12	3.23	0.76
Tm	0.09	0.06	0.09	0.05	0.11	0.1	0.15	0.05	0.05	0.05	0.58	0.16
Yb	0.34	0.43	0.48	0.17	1.4	0.4	0.16	0.25	0.05	0.16	3.36	0.48
Lu	0.15	0.16	0.04	0.25	0.05	0.1	0.04	0.02	0.11	0.02	0.48	0.13
ΣLREE	55.5	6.28	16.6	16.5	19.2	10.3	3.16	3.79	2.55	2.39	200	23.6
ΣHREE	2.24	1.08	1.65	0.59	2.54	0.9	0.5	0.53	0.2	0.41	8.74	3.21
ΣREE	58.1	7.67	18.2	17.5	22.9	11.7	3.93	4.57	2.75	2.89	214	26.8
Eu/Eu*	1.3	1.5	0.8	1.23	1.6	1.3	1	1	3.24	0.8	3.24	1.5
(La/Sm) <sub>N</sub>	7.15	2.3	6.4	5.3	3.8	4.2	3.5	4.5	7	1.7	11.3	5.3
(Gd/Yb) <sub>N</sub>	4.9	1.7	1.5	3.5	0.8	1	1.6	1.5	1	0.3	4.9	1.4
(La/Yb) <sub>N</sub>	42.1	3	12.1	21	3	5.3	4.4	3.6	7	0.8	42.1	7.7
(Sm/Yb) <sub>N</sub>	4.1	1.5	2.1	5.2	1.0	1.4	1.3	0.98	2.2	0.6	5.2	1.6

TRACE ELEMENTS -ITABIRITE															
ppm	IIT	IIV	ICO	IPI	ICM	ITA	IPC	IMF	ITO	IGS	ICE	ICH	MIN	MAX	AVG
V	16	9.0	18.0	9.0	10.0	47.0	12.0	55.0	2.5	7.0	21.0	41.0	2.5	55.0	20.6
Co	2.3	43.9	29.7	34.3	34.9	2.1	1.1	1.7	20.5	25.6	31.9	31.3	1.1	43.9	21.6
Ni	22.3	3.2	3.3	3.6	6.8	42.1	17.4	33.4	1.3	0.8	1.2	0.4	0.4	42.1	11.3
Cu	3.8	0.7	0.1	0.4	19.8	8.0	3.6	6.6	0.7	0.7	0.4	2.0	0.1	19.8	3.9
Zn	2.0	2.0	1.0	1.0	8.0	3.0	2.0	3.0	1.0	0.1	1.0	0.1	0.1	8.0	2.0
Rb	0.3	0.3	0.6	0.3	0.3	1.2	0.3	1.1	0.3	0.3	0.3	0.3	0.3	1.2	0.5
Sr	0.8	10.3	2.8	0.9	21.8	3.9	1.7	4.5	0.6	3.1	2.8	2.1	0.5	21.8	4.6
Y	2.6	7.9	4.0	2.5	8.4	5.8	1.2	4.2	3.3	14.1	1.8	3.9	1.2	14.1	5.0
Zr	1.7	1.4	2.2	0.9	13.5	1.5	1.2	8.1	1.4	0.7	1.4	2.5	0.7	13.5	3.0
Nb	2.5	0.3	0.3	0.3	0.7	4.7	2.0	3.8	0.3	0.3	0.3	0.3	0.3	4.7	1.3
Ba	2.3	3.5	19.2	0.3	3.6	17.1	5.6	66.1	5.7	13.3	1.3	21.7	0.3	66.1	13.3
Hf	0.3	0.3	0.3	0.3	0.3	0.3	0.3	0.3	0.3	0.3	0.3	0.3	0.3	0.3	0.3
Ta	0.1	0.5	0.5	0.4	0.3	0.1	0.1	0.1	0.3	0.3	0.5	0.4	0.1	0.5	0.3
ΣTE	57	83.3	82	54.2	128	136.8	48.5	187.9	38.1	56.6	64.2	106.3	38.1	187.9	57.8
ITABIRITE (REE Concentration)															
ppm	IIT	IIV	ICO	IPI	ICM	ITA	IPC	IMF	ITO	IGS	ICE	ICH	MIN	MAX	AVG
La	1	1.3	1.5	0.5	4.2	4.5	0.6	2.8	1.5	15.1	0.5	0.8	0.5	15.1	3.75
Ce	1.7	2.6	2.9	0.6	5.9	7.5	0.8	6.2	1.6	19.6	1.2	1.4	0.6	19.6	5.15
Pr	0.2	0.36	0.45	0.1	0.73	0.8	0.15	0.95	0.25	4.12	0.16	0.24	0.1	4.12	0.909
Nd	0.5	1.9	2.1	0.5	2.8	3.6	<0.4	4	0.9	19.8	0.6	1.3	0.5	19.8	4.48
Sm	0.2	0.5	0.5	0.1	0.7	0.5	0.1	0.9	0.1	3.9	0.3	0.5	0.1	0.9	0.43
Eu	<0.05	0.17	0.16	<0.05	0.18	0.18	<0.05	0.19	<0.05	1.27	0.13	0.14	0.13	1.27	0.378
Gd	0.23	0.62	0.58	0.19	0.59	0.57	0.06	0.86	0.28	3.49	0.24	0.8	0.06	3.49	0.86
Tb	0.03	0.11	0.19	0.03	0.13	0.15	0.03	0.11	0.07	0.52	0.05	0.1	0.03	0.52	0.14
Dy	0.23	0.53	0.58	0.41	0.92	0.75	<0.05	0.54	0.32	2.45	0.19	0.58	0.19	2.45	0.78
Ho	0.06	0.16	0.13	0.09	0.21	0.19	<0.05	0.09	0.08	0.41	<0.05	0.12	0.06	0.41	0.16
Er	0.21	0.47	0.65	0.32	0.71	0.49	0.08	0.31	0.23	1.02	0.2	0.24	0.08	1.02	0.44
Tm	<0.05	0.08	0.15	0.05	0.1	0.07	<0.05	0.05	0.07	0.16	<0.05	<0.05	0.05	0.16	0.095
Yb	0.24	0.53	0.32	0.52	0.63	0.37	0.15	0.31	0.29	0.93	<0.05	0.29	0.15	0.93	0.43
Lu	0.12	0.04	0.05	0.08	0.08	0.04	0.08	0.13	0.1	0.04	0.08	0.14	0.04	0.14	0.08
ΣLREE	3.83	7.45	8.39	2.09	15.18	17.73	1.71	15.9	4.63	63.83	3.13	5.18	1.71	53.83	15.23
ΣHREE	0.86	1.92	2.09	1.6	2.65	1.91	0.34	1.44	1.16	5.01	0.47	1.47	0.34	5.01	1.68
ΣREE	4.72	9.37	10.51	3.59	17.96	19.79	2.05	17.45	5.79	68.91	3.65	6.65	2.59	69.91	16.91
Eu/Eu*	1.1	1.4	1.2	2	0.5	1.2	1.5	0.5	3	1	3.9	2	1	3	1.6
(La/Sm) <sub>N</sub>	5	2.5	2.7	6	5	7.5	5	3.1	15	3.9	1.7	1.6	1.6	15	5.8
(Gd/Yb) <sub>N</sub>	1	1.2	2	0.6	1.2	1.5	0.5	3	1	3.9	2	2.7	0.6	3.9	1.9
(La/Yb) <sub>N</sub>	5	2.5	5.3	3	7	11.3	3	9.3	5	16.8	5	2.7	2.6	16.8	7.3
(Sm/Yb) <sub>N</sub>	0.5	1.5	2.3	0.7	1.3	1.8	0.8	3.2	0.5	4.7	6.7	1.9	0.5	4.7	2.1

and Ta (0.1-0.3 ppm). Ba is an important trace element with concentration relatively higher than the last group of trace elements (Rb-Ta) but with large scattering of values (0.3-35.2 ppm). Sample HAI2 has high values of some trace elements such as V, Co, Y, Sr, Ba and Zr.

Similarly to hematitite, the concentrations of trace elements in the itabirite show a wide

range of concentrations (Table 1). Their total abundance is in average 87.8 ppm. V and Co are the most abundant trace elements. V content has an average of 20.6 ppm and concentration within the limits 2.5 and 55 ppm (Table 1). Co concentrations have high average values around 21.6 ppm. Ba also shows a wide limit of concentration between 0.3- 6.1 ppm, having an average of 13.3 ppm. Hf and Ta present very low concentrations in the itabirite with average



of 0.3 ppm. The average content of Rb (0.5 ppm) is more or less similar to that obtained for Hf and Ta. The other trace elements, Cu (min. and max.: 0.1-19.8 ppm), Zn (0.1-8 ppm), Sr (0.5-21.8 ppm), Y (1.2-14.1 ppm), Zr (0.7-13.5 ppm) and Nb (0.3-4.7 ppm) have low average contents with high variability.

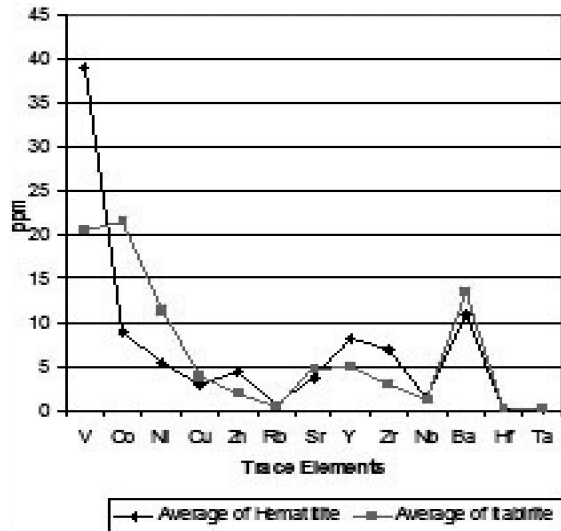


**Figure 3:** Plot of the average concentration of trace-elements of the hematitite and itabirite samples.

Similarly to the hematitite, there are highly anomalous values of trace elements such as V, Ni, Co, Y and Ba mostly in samples collected from the eastern domain of QF region. The analysed data indicate an increase of some trace elements of mantle derived sources of some samples along with a decrease of trace elements of felsic affinity (especially Rb and Hf) mostly for those samples located in the eastern domain.

**Rare earth elements (REEs)**

Studies on rare-earth elements (REEs) distribution of iron-formations have provided valuable insight on the evolution of the terrestrial atmosphere-hydrosphere-lithosphere system and lead to the development of general models of IF genesis.

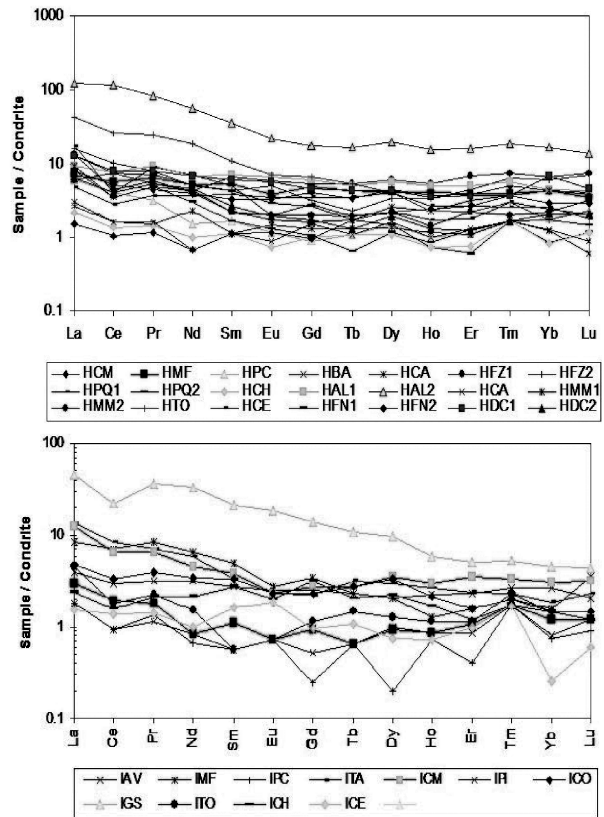


**Figure 4:** Chondrite (after Evensen *et al.*, 1978) normalized pattern of rare earth elements (REE) calculated for the hematitite samples (a) and itabirite samples (b).

In hematitite samples,  $\Sigma$ REE contents are in an average of 24.9 ppm and the contents of light REE (LREE; La to Eu) in all samples varies between 2.2 and 195.1 ppm and are 4 times higher than the heavy REE (HREE; Gd to Lu) ranges from 0.7 to 18.9 ppm. In itabirite samples the total content of REE is in average around 19.8 ppm (Table 1).

The abundance of LREE is appr. 12.1 ppm, ranging from 2.2 to 63.8 ppm, whereas the total content of HREE sums up 2.5 ppm (0.7-9.2 ppm). All samples show increase in the LREE content to HREE content which is more pronounced in the hematitite samples. To evaluate the degree of fractionation of LREE to HREE, REE's were normalized to chondrites (CN) (Evensen *et al.*, 1978). The shape of the distribution of  $(REE)_{CN}$  show nearly horizontal patterns with relatively slight high fractionation of LREE to HREE and similar for both hematitite and itabirite (Figure 4). LREE fractionation was determined by the ratio  $(La/Sm)_{CN}$  and

HREE fractionation was obtained by the ratio  $(Gd/Yb)_{CN}$ . In the hematite LREE fractionation ratio  $(La/Sm)_{CN}$  presents an average of 5.3 (Table 1) whereas the ratio  $(Gd/Yb)_{CN}$  has an average value of 1.4. For the itabirite, the  $(La/Sm)_{CN}$  ratio presents an average of 5.8 and  $(Gd/Yb)_{CN}$  is in average of 1.9 (Table 1). The bulk fractionation degree of LREE to HREE was determined for the hematite and itabirite samples by the ratio of  $(La/Yb)_{CN}$  which gave an average of 7.7 and 7.3 respectively. This ratio reaches high values in some samples mostly those located in the eastern domain of QF region. The medium values of Eu anomaly ( $Eu/Eu^*$ ) are slight positive and variable in all the samples collected in QF mines.

**DISCUSSION**

**a) Elements distribution in iron ores samples**

The two ore samples analysed in this paper, the hematite and the itabirite have relatively simple mineralogy. The dominant minerals are hematite and quartz. Magnetite appears in minor quantities, mostly in iron rocks from the west domain of the QF.

We selected for the analyses only unaltered samples (from deep open pit mine). In the east/southeast boundary of the QF, tourmaline may occur scattered in the iron formation rocks in trace amounts (< 1%). All these aspects result in a very simple chemical composition of the iron oxide formations in the QF region.

This study indicates that iron formation in the QF region share some characteristics with other known IFs around the world. The banding of the itabirite in the QF is similar in shape to the Hamersley Basin in Australia, the Orissa region of India and those of South Africa (James, 1954; Cole, 1981).

In relation to trace elements, the mean values for hematite and itabirite are comparable to the trace elements concentration averages of IFs reported in Spier *et al.* (2007) and in Lindenmayer *et al.* (2001) (Klein and Ladeira 2000) (Table. 3). The data analysed have lower concentrations in comparison to itabirite of Klein and Ladeira (2000) but more or less similar to the itabirite of Spier *et al.* (2007). However when compared with other IFs in the world, both hematite and itabirite show lower

**Table 2:** Average of trace element contents in iron formation of this study compared with some iron formations of the QF region and from other parts of the world.

ppm	QF	This Study		QF <sup>a</sup>		QF <sup>b</sup>		Carajás <sup>c</sup>	Superior <sup>d</sup>	Algoma <sup>e</sup>	Nigeria <sup>f</sup>	Orissa India <sup>g</sup>
	Hematite	Quartz	Itabirite	Quartz	Itabirite	Quartz	Itabirite	BIF	BIF	BIF	BIF	BIF
V	39		20.6		22.6	-	-	-	30.0	97.0	44.0	30.0
Co	9		21.6		-	249.0	-	-	27.0	38.0	100.0	35.0
Ni	5.5		11.3		10.5	20.0	< 20	32.0	83.0	< 10	< 10	15.0
Cu	2.9		3.9		< 1.0	33.8	-	10.0	96.0	< 10	< 10	10.0
Zn	4.4		2		-	42.3	-	2.0	33.0	26.0	26.0	-
Rb	0.6		0.5		< 1.0	32.9	1_9	-	-	-	20.0	-
Sr	3.7		4.6		5.0	10.3	< 5	42.0	83.0	51.0	51.0	15.0
Y	8.2		5		3.9	4.8	< 3	41.0	54.0	22.0	22.0	-
Zr	7		3		12.0	2.5	0.3-30	60.0	84.0	60.0	60.0	10.0
Nb	1.4		1.3		0.8	6.4	< 0.5-13	-	-	-	5.0	-
Ba	10.8		13.3		15.4	55.4	10_29	180.0	170.0	293.0	293.0	70.0
Hf	0.3		0.3		< 0.1	0.1	-	-	-	-	-	-
Ta	0.1		0.3		-	0.1	-	-	-	-	-	-
ΣTE	92.6		87.8		8.2	457.3	8.1	424.0	738.0	621.0	621.0	185.0

a Paleoproterozoic banded iron formation (Itabirite of Cauê Fm.) (Spier *et al.*, 2007)

b Itabirite of Cauê Fm. (Klein and Ladeira 2000)

c Jaspilite of Carajás Formation (Lindenmayer *et al.*, 2001)

d Lake superior silicate facies iron-formation (Animikie) (Gross and Macleod, 1980, table 3)

e Algoma oxide facies iron-formation (Gross and Macleod, 1980, table 3)

f Maru iron formation (oxide facies) (Adeloya, 1998)

g Orissa iron-formation (oxide facies), India (Majumber *et al.*, 1982, table 3)

**Table 3:** Average of rare earth element contents in iron formation of this study compared with some iron formations of the QF region and from other parts of the world.

ppm	QF	This Study	QF <sup>a</sup>	QF <sup>b</sup>	Hamersley <sup>c</sup>	Transvaal <sup>d</sup>	Surgur belt <sup>e</sup>
	Hematite	Quartz Itabirite	Quartz Itabirite	Quartz Itabirite	BIF	BIF	BIF
La	6.51	3.75	1.4	1.87	0.22	7	1.37
Ce	13.96	5.15	2.32	2.38	0.54	12.71	2.73
Pr	1.45	0.9	1.59	1.9	0.2	5.49	1.46
Nd	5.45	4.48	0.32	ND	0.06	1.47	3.23
Sm	1.22	0.43	0.43	0.25	0.08	1.13	3.05
Eu	0.34	0.37	0.54	0.25	0.14	1.512	0.3
Gd	1.04	0.86	0.3	0.15	0.09	0.85	0.22
Tb	0.17	0.14	0.35	ND	0.08	0.85	0.23
Dy	1.04	0.78	0.15	0.17	0.02	0.33	1.65
Ho	0.25	0.16	0.12	ND	ND	0.26	0.07
Er	0.76	0.44	0.09	ND	ND	0.19	0.06
Tm	0.16	0.09	0.56	ND	0.1	1.16	0.34
Yb	0.48	0.43	0.05	ND	ND	0.11	0.03
Lu	0.13	0.08	0.05	0.02	0.02	0.13	0.03
∑LREE	23.64	15.23	0.05	6.04	1.1	27.8	11.84
∑HREE	3.21	1.68	2.21	0.59	0.45	5.04	2.93
∑REE	26.85	16.91	8.26	6.99	1.55	32.85	14.78
(La/Yb) <sub>N</sub>	7.7	7.3	0.51	1.52	1.87	0.88	0.94
(Eu/Eu) <sub>N</sub>	1.5	1.6	1.49	3.18	1.33	1.45	2.13

a Paleoproterozoic banded iron formation (Itabirite of Cauê Fm.) (Spier et al, 2007)

b Jaspilite of Carajas Formation (Macambira and Schrank, 2002))

c Hamersley banded formation (Glikson et al. 2004)

d Transvaal Supergroup, Kuruman BIF (oxide facies) (Klein and Beukes, 1989)

e Surgur Belt, India, (Kato et al., 1996)

average contents of trace elements (Table 2). Also the ore samples have lower concentration levels of Ba than the data analysed by Klein and Ladeira (2000) and Spier *et al.* (2007) in the QF region as well as the Ba concentration for all data around the world.. The data of mantle affinity for the Lake Superior types are higher than those of itabirite of QF. The data of V for hematite are higher than for itabirite, but are not so different from the data of samples from Nigeria. In comparison to the data of Algoma, trace element values are much higher than the data of studied ore of QF region. The data of trace elements in India are much higher than the data of the studied ore samples except in the value of V element which is more or less similar. The analysed data show lower concentration for Ni and Cu in comparison with data analysed for QF region as well as BIFs around the world.

REE inventory in the QF iron formations is in the same range of variation to that found in IFs around the world (Figure 5). The majority of analysed samples display similar REE signature characteristics as do other IFs of similar age proposed by the work of (Bau and Müller, 1993) where they indicated the IFs independent from their provenance, age, metamorphic grade display a similar REE signature of  $(La/Sm)_{CN} > 1$ ,  $(Eu/Eu^*)_{CN} > 1$  which is compatible with our data analysed (Table.1).

The sum of REEs of the analysed samples of this study is higher than the itabirite analysed by Spier (2007) and jaspilites of Carajás formation (Macambira Shrank and, 2002). In comparison to the other BIFs around the world, the itabirite of this study show values more or less similar to REEs contents to the Surgur belt (Kato *et*

*al.*, 1996) and lower than BIF of Kuruman oxide facies (Klein and Beukes, 1989) (Table 3).

In average the total content of REEs are relatively low with slight high degree of fractionation of LREE to HREE. The chondrite enrichment ratio  $(La/Yb)_N$  show high values in comparison to other banded iron formations around the world. The work proposed by (Derry and Jacobsen, 1990) indicated when the ratio of  $(La/Yb)_N > 1$ , this mean small distance to hydrothermal source. But when the ratio of  $(La/Yb)_N < 1$ , this mean long distance to the source. Our analysed data show high values of  $(La/Yb)_N$  ratio in the majority of samples mostly those located in the eastern domain and this result indicate a small distance to the hydrothermal source of iron.

#### **b) Considerations on the genesis of hematite and itabirite**

The iron ore samples analysed in this study are characterized by their relatively pure composition. The amount of Fe and silica in this rock is larger than 98 weight %. In the hematite type silica is less than 1% in weight, making these rocks a nearly pure hematite iron ore. Even for the itabirite the total concentration of total Fe and SiO<sub>2</sub> is in average higher than 98.5%. The study area was affected by geologic processes of deformation and metamorphism that transformed the original BIFs into the itabirites observed today. These factors making the geochemical scenario get complicated and genesis of iron ore in the QF region is still debated.

The chondrite-normalized REE pattern of all samples characterized by enrichment of light REE (LREE) relative to heavy REE (HREE) (Figure 4) coupled with slight positive Eu anomalies (average value of 1.5 and 1.6 for hematite and itabirite respectively). These features closely resemble REE distribution in the present day hydrothermal fluids added at mid ocean-ridge vent sites indicated by the work

of (Bau *et al.* 1995; Bau and Dulsky, 1996) suggest the source for iron was result of deep ocean hydrothermal activity admixed with sea water.

Although metamorphism increases from western domain to eastern domain in the QF region but the concentrations of trace and rare earth elements are dispersed and appeared in anomalous values especially in the eastern domain of QF region.

The data of this work show anomalous values of trace elements (mainly in transition metals) and rare earth elements (LREE) were recorded for the samples collected in some mines of QF region like in Algeria, Dois Córregos, Chacrinha, Periquito and Conceição in comparison to other samples.

V, Co and Ni are considered to be relatively mobile in aqueous fluids, this mean that these elements will be unstable in hydrothermal, sea-floor weathering and up to medium metamorphic grades (mid amphibolite facies) (Rollinson, 1993).

The study area reach medium grade of metamorphism (600°C) and the mineralization of Fe could be occurred during this stage (supergene leaching of Quartz and carbonate) as well as remobilization of iron occurred in minor scale creating high grade hematite ore. This indicated by high value of V element, this element usually concentrate during the enrichment processes and enriched in residual form during the process of mineralization of Fe because it is very sensitive to the condition of oxi-reduction and less mobile in oxidant conditions (Schwertmann *et al.*, 1994; Brugger *et al.*, 2000). Besides the anomalous values of Ba and Co elements that accelerate fluid migration in hydrothermal mineralization (Goldschmidt, 1954). These features could be strong indications of contribution of supergene enrichment attributed the genesis of hematite and itabirite to the

hydrothermal metasomatism of the original BIF during a hypogene enrichment.

This model is compatible with the model described by Beukes *et al.*, (2002). They studied the high grade iron ore of Águas Claras mine in QF region and attributed the genesis of itabirite to supergene modified hydrothermal metasomatism developed from the replacement of the original chert bands in iron formation by carbonates during hypogene enrichment. Moreover our work is compatible with the model proposed by (Taylor *et al.*, 2001; Dalstra and Guedes, 2004 ) for Hamersley Province, Western Australia, explaining the origin of high grade iron ores related to hydrothermal silica dissolution and introduction of carbonate in the original iron formation followed by supergene leaching of carbonates creating high grade hematite ore.

The chondrite enrichment ratio of  $(La/Yb)_N$  show high values in samples collected in Algeria mine and Itabira area mines suggesting that the source might be located near the eastern domain of QF region.

### **CONCLUSIONS**

The iron ore samples (oxide lithofacies) collected from the QF region consist mainly of hematite, magnetite and quartz. Variety of minerals such as tourmaline may also be found in the eastern side of the

QF area. The analysed samples are of two types: high grade hematite (hematite) and itabirite. Hematite has more than 98% of Fe whereas the itabirite have varied contents of iron and silica in average higher than 99%. The trace elements of all collected samples present considerable variability in all samples with anomalous values of V, Co, Ni, Y, Ba, Zr mostly from the area located in the eastern domain of QF region in relation to other samples.

The samples show a low REE abundances and slight high fractionation ratio of LREE to HREE besides slight positive Eu anomalies. This pattern is similar to some BIFs around the world suggesting the contribution of a hydrothermal source of iron ore.

The metamorphism caused hydrothermal alteration of the rock chemical compositions supporting the supergene enrichment model especially for the eastern domain of QF region indicated by anomalous values of trace and rare earth elements coupled with high values of  $(La/Yb)_N$  ratio suggest that the source of iron located near to Itabira region.

### **ACKNOWLEDGMENT**

Special thank goes to all my colleagues in Micro-Lab- UFOP for their helping and valuable discussion.

### **REFERENCES**

- ADEKOYA, J.A. (1998) The geology and geochemistry of the Maru Banded Iron-Formation, northwestern Nigeria. *Journal of African Earth Sciences*, **27**: 241-257.
- ALIBERT, C. & MCCULLOCH, M.T. (1993) Rare earth element and neodymium isotopic compositions of the banded iron-formations and associated shales from Hamersley, Western Australia. *Geochimica et Cosmochimica Acta* **57**: 187-204.

- ALKMIM, F.F. & MARSHAK, S. (1998). Transamazonian Orogeny in the Southern São Francisco Craton Region, Minas Gerais, Brazil: evidence for Paleoproterozoic collision and collapse in the Quadrilátero Ferrífero. *Precambrian Research*, **90**: 29-58.
- BAU, M. & MÖLLER, P. (1993) Rare earth element systematics of the chemically precipitated component in Early Precambrian iron formations and the evolution of the terrestrial atmosphere hydrosphere- lithosphere system. *Geochim. Et Cosmochim. Acta*, **57**: 2239-2249.
- BEUKES, N.J.; GUTZMER, J.; MUKHOPADHYAY, J. (2002). The geology and genesis of high-grade iron ore deposits, Iron Ore. Australasian Institute of Mining and Metallurgy, Perth, pp. 23-29.
- BAU, M.; DULSKI, P.; MÖLLER, P. (1995) Yttrium and holmium in South Pacific seawater: vertical distribution and possible fractionation mechanisms. *Chemie der Erde*, **55**: 1-15.
- BAU, M. & DULSKI, P. (1996) Distribution of Y and rare-earth elements in the Penge and Kuruman Iron-Formations, Transvaal Supergroup, South Africa. *Precambrian Research*, **79**: 37-55.
- BRUGGER, J. (2000) Origin and distribution of some trace elements in metamorphosed Fe-Mn deposits, Val Ferrera, Eastern Swiss Alps, *Canadian Minerologist*, **38**: 1075-1101.
- CHEMALE, F.JR.; ROSIÈRE, C.A.; ENDO, I. (1994) The tectonic evolution of the Quadrilátero Ferrífero, Minas Gerais, Brazil. *Precambrian Research*, **65**: 25-54.
- COLE, M.J. (1981) Archean banded iron-formations, Yilgarn Block, Western Australia. *Economic Geology*, **76**: 1954-1974.
- CORDANI, U.G.; KAWASHITA, K.; MÜLLER, G.; QUADE, H.; REIMER, V.; ROESER, H. (1980) Interpretação tectônica e petrológica de dados geocronológicos do embasamento na borda sudeste do Quadrilátero Ferrífero. *Anais da Academia Brasileira de Ciências*, **52**: 785-799.
- DERRY, L.A. & JACOBSEN, S.B. (1990) The chemical evolution of Precambrian seawater: Evidence from REEs in banded iron formations. *Geochim. et Cosmochim. Acta*, **54**: 2965-2977.
- DORR J.V.N. & BARBOSA A.L.M. (1963) Geology and ore deposits of the Itabira District, Minas Gerais, Brazil. U. S. Geological Survey Prof. Paper 341-C. Washington, DC, 110p.
- DORR II, J.V.N. (1969) Physiographic, Stratigraphic and Structural Development of the Quadrilátero Ferrífero, Minas Gerais, Brazil. U.S. Geological Survey Professional Paper 641-A, 42p.
- EVENSEN, N.M.; HAMILTON, P.J.; O'NIONS, R.K. (1978) Rare earth abundances in chondritic meteorites, *Geochimica et Cosmochimica Acta*, **42**: 1199-1212.
- GLIKSON, A.Y. & ALLEN, C. (2004) Iridium anomalies and fractionated elements pattern in impact ejecta, Brockman iron formation, Hamersley Basin, Western Australia: evidence for a major a sterio impact in simatic crustal regions of the Early Proterozoic Earth. *Earth and Planetary Science Letters*, **220**: 247-264.

- GROSS, G.A. (1980) A classification of iron formations based on depositional environments. *Canadian Mineralogist*, **18**: 215-222.
- GROSS, G.A. & MACLEOD, C.R. (1980) A preliminary assessment of the chemical composition of iron formations in Canada. *Canadian Mineralogist*, **16**: 223-229.
- GOLDSCHMIDT, V.M. *Geochemistry the international series of monographs on physics*, part 1, 1954, 730p.
- DALSTRA, H.J. & GUEDES, S. (2004) Giant hydrothermal hematite deposits with Mg-Fe metasomatism: a comparison of the Carajás, Hamersley, and other iron mines. *Econ. Geol.*, **99**: 1793-1800.
- HERZ, N. (1978). *Metamorphic rocks of the Quadrilátero Ferrífero, Minas Gerais, Brazil*. U.S.G.S. Professional Paper 641-C. U.S. Geological Survey, U.S.A., p. C1-C81.
- JAMES, H.L. (1954) Sedimentary facies of iron-formations. *Econ. Geol.*, **49**: 235-293.
- KATO, Y.; TAKANORI, K.; TAKASHI, K.; KUNUGIZA, K.; SWAMY, N.S. (1996) Rare-earth element geochemistry of banded iron formations and associated amphibolite from the Sargur belts, south India. *Journal of Southeast Asian Earth Sciences*, **14**: 161-164.
- KLEIN, C. & LADEIRA, E.A. (2000) Geochemistry and petrology of some Proterozoic banded iron-formations of the Quadrilátero Ferrífero, Minas Gerais, Brazil. *Economic Geology*, **95**: 405-428.
- KLEIN, C. & BEUKES, N.J. (1989) Geochemistry and sedimentary of a facies transition from limestone to iron formation deposition in the Early Proterozoic Transvaal Supergroup, South Africa. *Economic Geology*, **84**: 1733-1774.
- LAGOEIRO, L. (1998) Transformation of Magnetite to Hematite and its influence on the dissolution of iron oxide minerals. *Journal of Metamorphic Geology, Gra-Bretanha*, **16**: 415-423.
- LINDENMAYER, Z.G.; LAUX, J.H.; TEIXEIRA, J.B.G. (2001). Considerações sobre a origem das formações ferríferas da formação Carajás, Serra dos Carajás. *Revista Brasileira de Geociências*, **31**: 21-28.
- MARSHAK, S. & ALKMIM, F.F. (1989). Proterozoic contraction/ extension tectonics of the southern São Francisco region, Minas Gerais, Brazil. *Tectonics*, **8**: 555–571.
- MAJUMDER, T.; HAKRABORTY, K.T.; BHATTACHARYYA, A. (1982) Geochemistry of banded iron formation, Orissa, India. *Mineralium Deposita* **17**: 107-118.
- MACAMBIRA, J.B. & SCHRANK, A. (2002) Químio-estratigrafia e evolução dos jaspelitos da Formação Carajás (PA). *Revista Brasileira de Geociências*, **32**: 567-578.
- MORALES, L.; LAGOEIRO L.; ENDO, I. (2008) Crystallographic fabric development along a folded polycrystalline hematite, *Journal of structural geology*, In press, 2008.

PIRES, F.R.M. (1995). Textural and mineralogical variations during the metamorphism of the Proterozoic Itabire Iron Formation in the Quadrilátero Ferrífero, Minas Gerais, Brazil. *Anais da Academia Brasileira de Ciências*, **67**: 77-105.

ROSIÈRE, C.A.; SIEMES, H.; QUADE, H; BROKMEIER, H.G.; JANSEN, E.M. (2001) Microstructures, textures and deformation mechanisms in hematite. *J Struct Geol.*, **23**:1429-1440.

ROLLINSON, H.R. (1993) *Using Geochemical Data: Evaluation, Presentation, Interpretation*. Longman, UK. 352 p.

SPIER, C.A.; OLIVEIRA, S.M.B.; SIAL, A.N.; RIOS, F.J. (2007). Geochemistry and genesis of the banded iron formations of the Cauê Formation, Quadrilátero Ferrífero, Minas Gerais, Brazil. *Precambrian Research*, **152**: 170-206.

SCHWERTMANN, U. & PFAB, G. (1994) Structural Vanadium in synthetic goethite. *Geochim. Cosmochim. Acta*, **58**: 4339-4352.

TAYLOR, D.; DALSTRA, H.J.; HARDING, A.E.; BROADBENT, G.C.; BARLEY, M.E. (2001) Genesis of high-grade hematite orebodies of Hamersley Province, Western Australia. *Econo.Geol.*, **96**: 837-873.